Spring 2013

Crystal Growth and Study of Unusual Magnetic Anomalies of a Low-Dimensional Iron(III) Oxy-Arsenates:

Liurukara D. Sanjeewa

Vasile O. Garlea

Pramod Kumar

Dino Sulejmanovic

Shiou-Jyh Hwu

Follow this and additional works at: https://tigerprints.clemson.edu/grads_symposium

Crystal Growth and Study of Negative Magnetic Anomalies of a Low Dimensional Iron(III) Oxy-Arsenate: $Rb_2Fe_2O(AsO_4)_2$

Liurukara D. Sanjeewa,[1] Vasile O. Garlea,[2] Pramod Kumar,[3] Dino Sulejmanovic,[1] Shiou-Jyh Hwu[1]

[1]Department of Chemistry, Clemson University, Clemson, SC 29634

[2]7 QCMD, Neutron Sciences Directorate, Oak Ridge National Laboratory, Oak Ridge, Tennessee 38831, USA

[3]Institute of Information Technology Allahabad, U.P. 211012, India

Introduction

Our most recent studies have been directed towards the synthesis of low-dimensional magnetic materials as these have drawn continued attention in condensed matter chemistry and physics, owing to their diverse electronic and magnetic properties. One example of such a family is $A_2Fe_2O(AsO_4)_2$ where A = K, Rb. Transition metal (TM) oxides sub-lattices that are structurally isolated and electronically insulated by closed shell nonmagnetic oxyanions (SiO_4^{4-}, PO_4^{3-}, AsO_4^{3-}) promoting stronger inter-chain magnetic interaction within the structurally isolated low dimensional TM−O chains. The magnetic properties are quite diverse for these systems, ranging from antiferro, ferri to ferromagnetic behavior and also the intriguing the complex magnetic anomalies such as magnetic frustration, step magnetization, negative magnetization. Studying the magnetic properties of such systems are benefited to the scientific community to understand the new physical phenomena involve in these unusual magnetic properties.

This demonstration mainly concentrated on the high temperature molten salt synthesis and magnetic characterization of $Rb_2Fe_2O(AsO_4)_2$. The magnetic susceptibility measurements show that, like originally reported for the Rb-analog, this compound undergoes a transition to a weak ferrimagnetic state near T_N = 22 K. Because of the availability of sizable single crystals, detailed orientation-dependent magnetic measurements were carried out. The results showed interesting magnetic anomalies such as step magnetization. Most notable feature here is the observation of negative magnetization for field cooling (ZC) and zero field cooling (ZFC) in very low applied fields and crossover of the FC and ZFC magnetization from negative to positive at relatively higher field. The magnetic properties of the title compound will be further explained using temperature dependent neutron powder diffraction (NPD) data.

Materials and Methods

Single Crystal Growth

KO_2 + Fe_2O_3 + As_2O_5 with 3(RbCl/RbI) eutectic flux

Heating program: heat to 800 °C, isotherm for 48 hrs, slowly cool to 300 °C at 0.1 °C/min, then furnace cool to room temperature. Sizable single crystals, ~ 3 mm in size in their longest axes can be grown employing slower cooling rate at 0.05 °C/min from 800 °C to 300 °C and applying a very high flux ratio (1:9 ratio between reactants and the flux).

Polycrystalline Sample

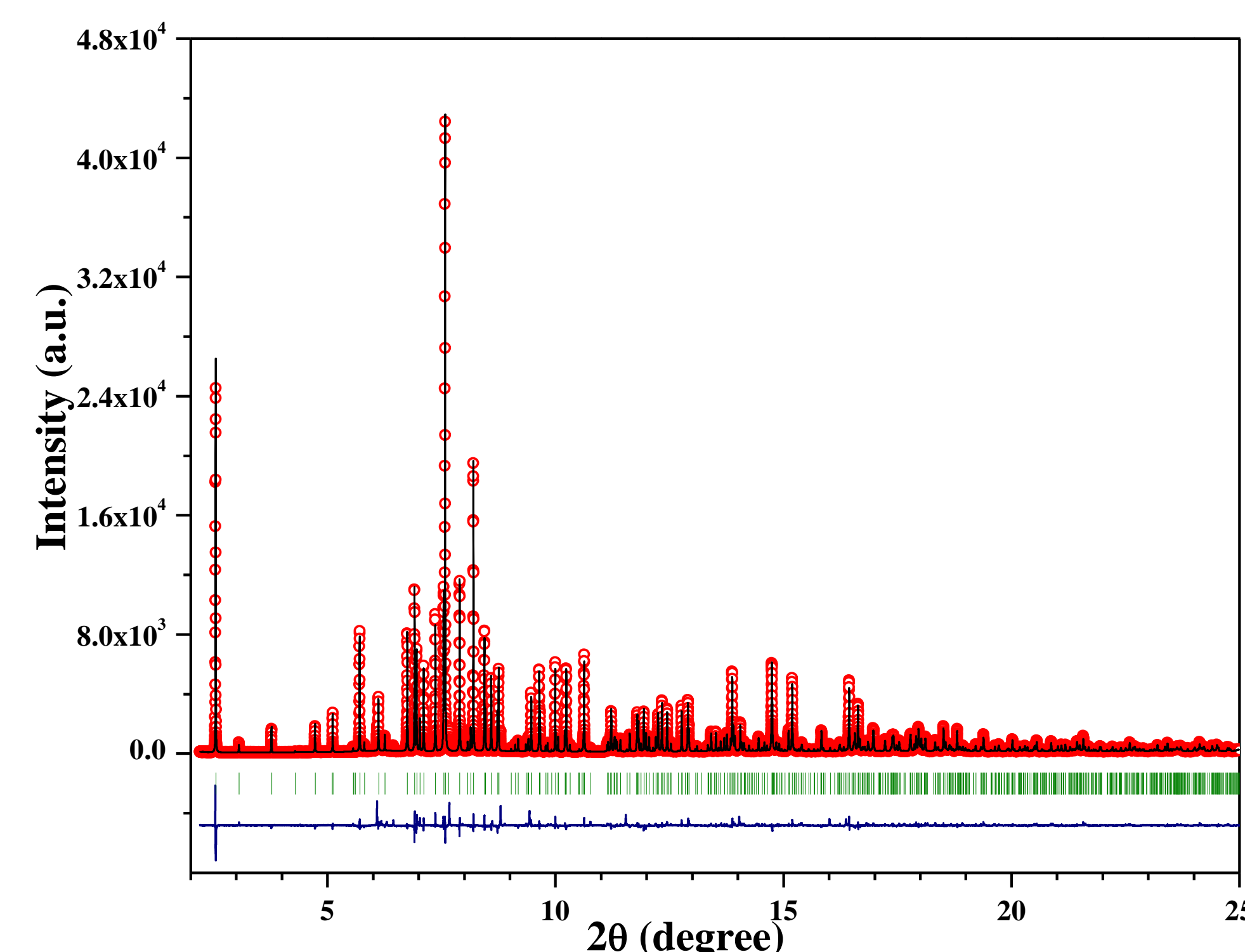Rb_2CO_3 + Fe_2O_3 + $2(NH_4)H_2AsO_4$ at 800 °C

Figure 1. High resolution synchrotron powder diffraction data were collected using beamline 11-BM at the Advanced Photon Source (APS), Argonne National Laboratory using an average wavelength of 0.413948 Å. The circles symbols and solid black line represent the observed and calculated patterns respectively. The difference curve is shown at the bottom (blue). Vertical bars indicate the expected Bragg peak positions according to the nuclear structure models depending on single crystals. The fitting residuals are χ^2 = 6.55, the weighted profile residual R_{wp} = 12.20 and the profile residual R_p = 7.68%.
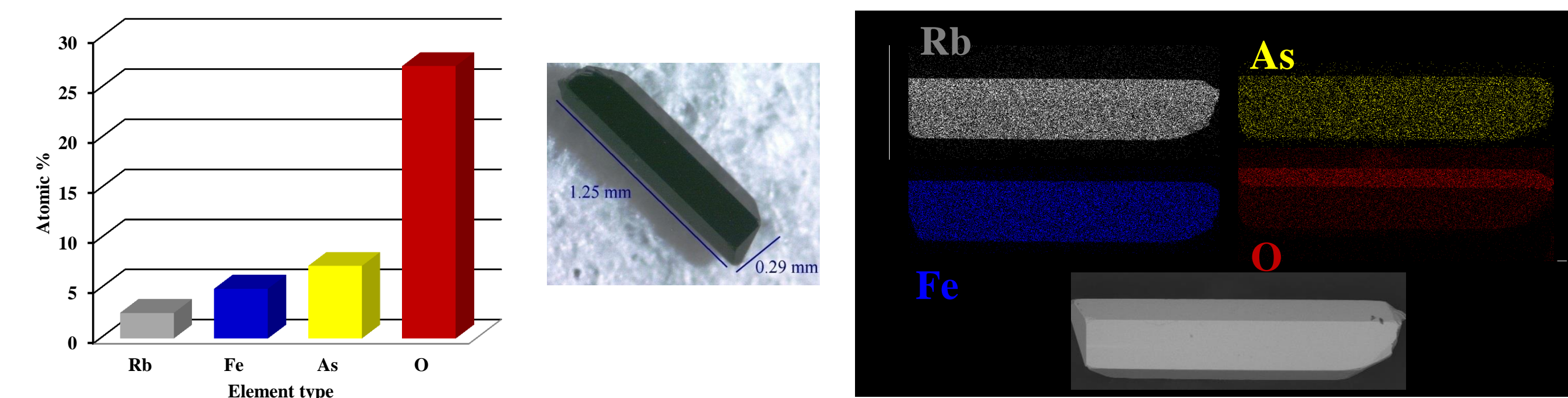

Figure 2. EDX of $Rb_2Fe_2O(AsO_4)_2$ single crystal shown in the SEM photo confirmed the presence of Rb, Fe, As and O.

Table 1. Crystallographic Data

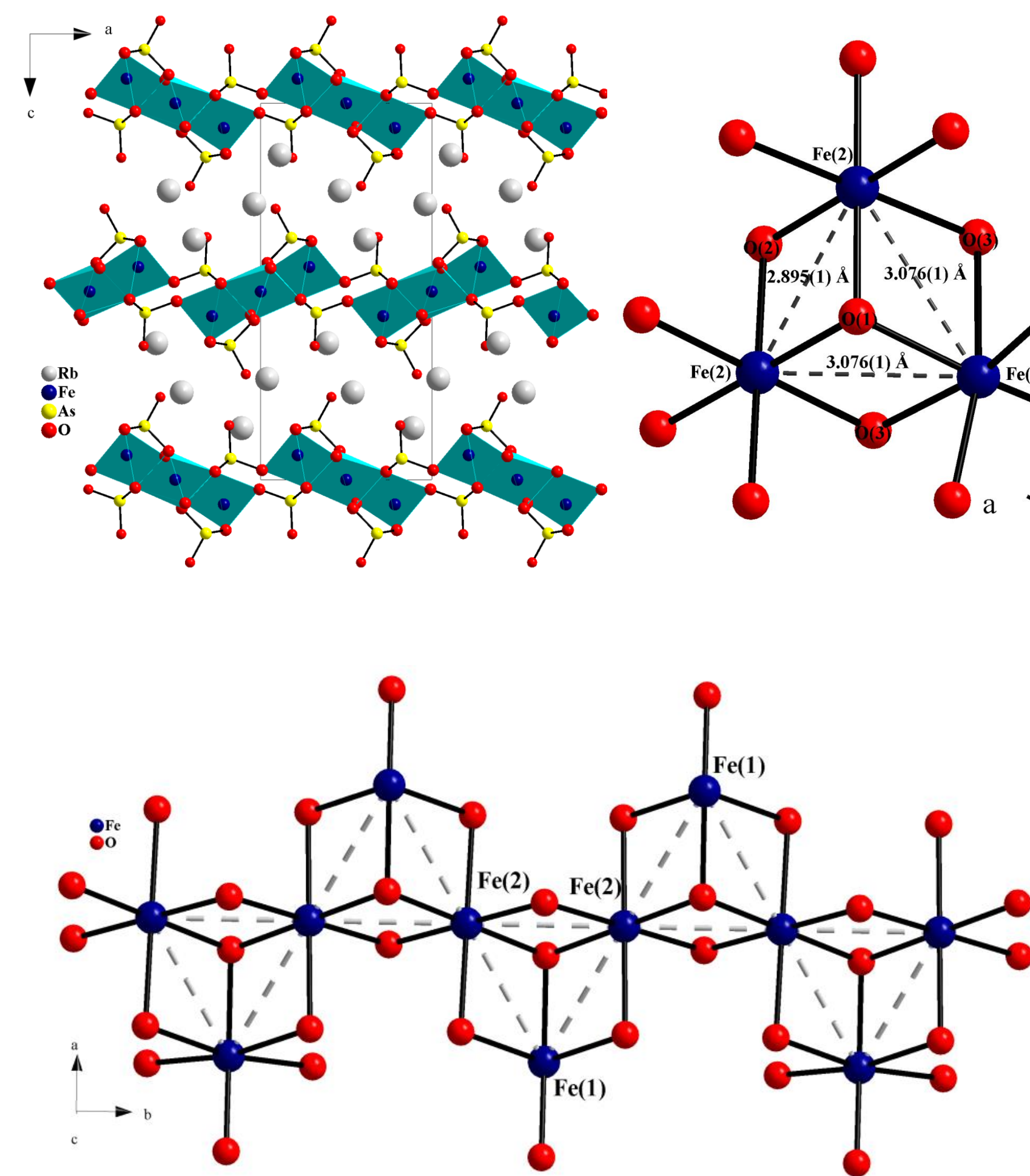|	
Empirical formula	$Rb_2Fe_2O(AsO_4)_2$
FW	576.48
Crystal System	orthorhombic
Crystal dimension, mm	0.42 x 0.05 x 0.04
Space Group, Z	*Pnma* (no. 62), 4
T, °C	27
a, Å	8.5331(7)
b, Å	5.7892(2)
c, Å	18.611(4)
V, Å³	919.(3)
μ (Mo Kα), mm⁻¹	20.845
d_{calc}, g cm⁻³	4.165
Data/restraints/parameters	894/0/86
Final R1, wR2[a] [I > 2σ(I)], GOF	0.0347/0.0936/1.038
Largest diff. peak/hole, e/ Å³	3.559/-2.333

Figure 3. (top right) Polyhedral view of the extended structure of $Rb_2Fe_2O(AsO_4)_2$ showing the structural confinement of the Fe-O-Fe chains. (top left) Triangular magnetic lattice of Fe^{3+}. (bottom) Partial structure of the $[Fe_4O_{14}]_\infty$ chain. There are two crystallographically distinct Fe^{3+} sites which are linked together to form a triangular based magnetic lattice, depicted by dashed grey lines. The nearest neighbor Fe distances for Fe(1)−Fe(2) and Fe(2)−Fe(2) are 3.076(3) Å and 2.895(3) Å respectively, resulting in nonequivalent exchange pathways within the chain.

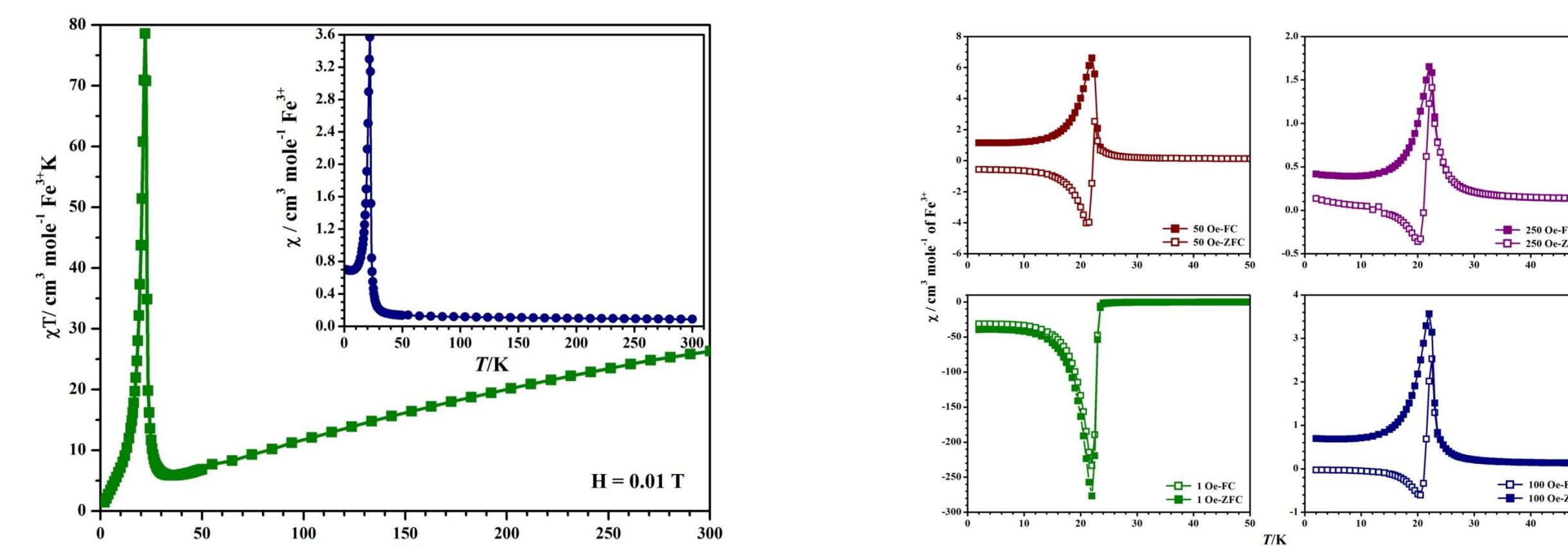## Magnetic Results and Neutron Powder Diffraction

Figure 4. Temperature-dependent magnetic susceptibility – χT vs. T; inset; χM vs. T at 0.01 T. and FC and ZFC curves indicate the negative magnetization at lower applied fields.
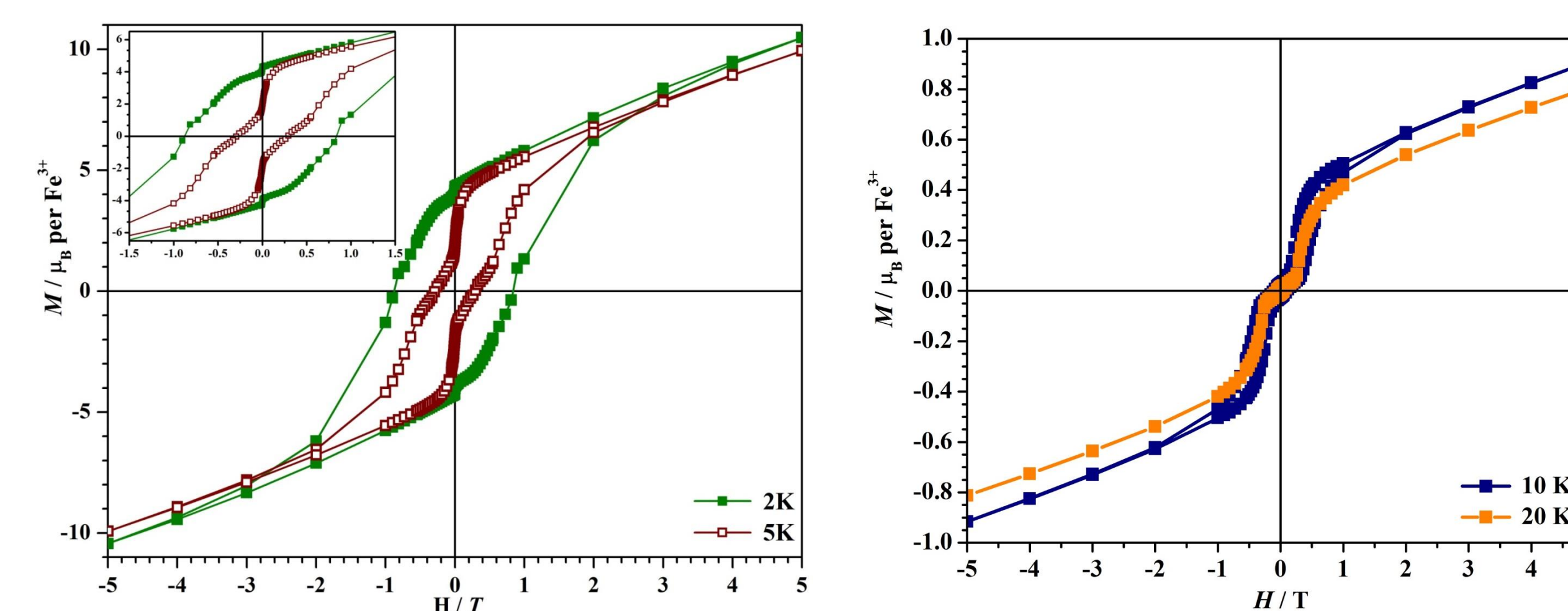

Figure 5. Magnetic field dependent of magnetization curves at 2 K and 5 K, 10 K and 20 K; ground single crystals.
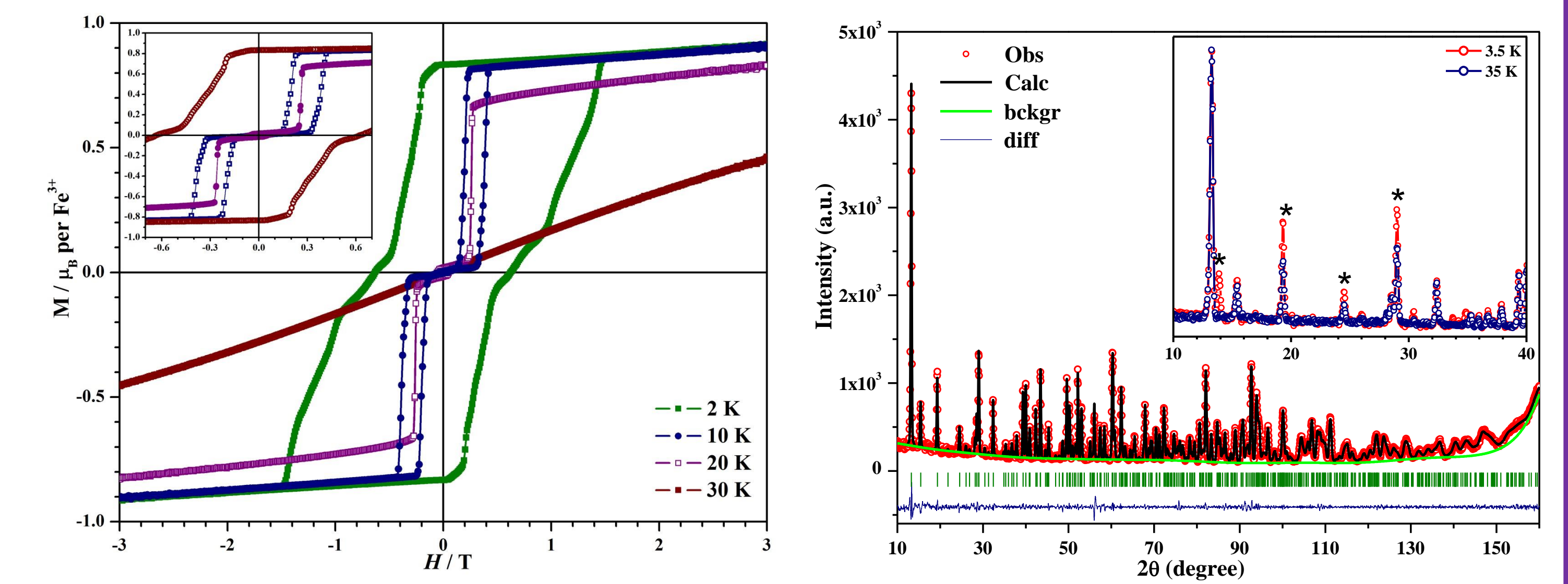

Figure 6. (left) Magnetic field dependent of magnetization curves for aligned single crystals. (right) NPD at 35 K; inset: showing magnetic peaks at 3.5 K.
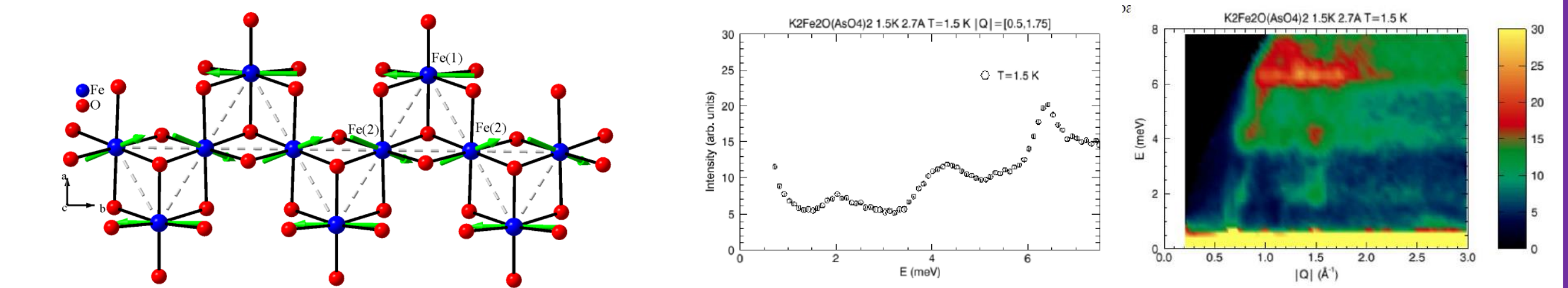

Figure 7. (left) Partial structure of the $[Fe_4O_{14}]_\infty$ chain. The green arrows represent the magnetic moments obtained from the NPD data at 3.5 K. (right) Powder inelastic data from DCS at 1.5 K. The data illustrate the presence of three distinct branches between 2, 4 and 8 meV.

Discussion and Conclusion

- Pseudo-low-dimensional magnetic solids display interesting magnetic phenomena. For example, quantum tunneling of magnetization (QTM), one of these unique magnetic phenomenon, is of great interest due to the potentials in quantum computing. SMMs (molecular solid) as well as the "spin-ice" pyrochlores $Dy_2Ti_2O_7$ and $Ho_2Ti_2O_7$, and $Ca_3Co_2O_6$ (extended solids) exhibit or are thought to exhibit QTM.

- $Rb_2Fe_2O(AsO_4)_2$, is a pseudo-one-dimensional, oxyanion-based magnetic insulator exhibits periodic arrays of electronically confined magnetic nanostructures that are separated by closed-shell, non-magnetic oxyanions, AsO_4^{3-}. These magnetic nanostructures or pseudo-one dimensional chains, $[Fe_4O_{14}]_\infty$, extend along the crystallographic b axis (Fig. 2).

- The temperature dependence of magnetic susceptibility for $Rb_2Fe_2O(AsO_4)_2$ was measured in an applied field of 0.01 T and 0.5 T. The least square fit of the high-temperature (50−300 K) data to the potentials in the Curie-Weiss equation, χ = C/(T - θ), where C is the Curie constant, and θ is the Weiss constant, yielded the best-fit values of C = 4.02(2) emu•K/mol and θ = -403.1(6) K. The calculated spin only value μ_{cacl} 5.7(5) μ_B is close to the expected spin only value for high spin d^5, 5.9μ_B.

- The field dependence of the magnetization was measured on oriented single crystals along their $[Fe_4O_{14}]_\infty$ chain axis, b (Figure 4) and show steps at 2, 10,and 20 K and at 30 K the hysteresis disappear.

- $Rb_2Fe_2O(AsO_4)_2$ shows negative magnetization in zero field cooling (ZFC) and field cooling (FC) measurements. Negative magnetization has been observed for materials showing thermally induced disorder of magnetic properties (*e.g.*, $LaSrCoRuO_6$) or for materials with inequivalent ferrimagnetically coupled sublattices with magnetization reversal (*e.g.*, RVO_3 where R = La, Nd, Sm, Gd, Er, and Yb).

- Neutron powder diffraction (NPD) data at various temperatures ranging from 3.3 K to 35 K indicated a lack of long range magnetic order and from the NPD data we have arrived a magnetic structure depicted in Figure 5. The first crystallographically distinct Fe site, Fe(1), has a magnetic moment that points directly along the b axis, while Fe(2) has a large b component and significantly smaller a and c components indicating a slight canting along the chain direction.

Acknowledgements

References

- a) Lawes, G.; Melot, B.; Page, K.; Ederer, C.; Hayward, M. A.; Proffen, T.; Seshadri, R. *Phys. Rev. B* 2006, 74, 024413; b) Dutta, D. P.; Manjanna, J.; Tyagi, A. K.; *J. Appl. Phys.* 2009, 106, 043915; c) Kumar, N.; Sundaresan, A. *Solid State Communications* 2010, 150, 1162-1164.
- a) Murthy, P. S. R.; Priolkar, K.R.; Bhobe, P.A.; Das, A.; Sarode, P. R.; Nigam, A. K. *Journal of Magnetism and Magnetic Materials* 2010, 322, 3704-3709; b) Priolkar, K. R.; Bhobe, P. A.; Sarode, P. R.; Nigam, A. K. *Journal of Magnetism and Magnetic Materials* 2011, 323, 822-828.
- Tung, L. D.; Lees, M. R.; Balakrishnan, G.; Paul, D. M. *Phys. Rev. B.* 2007, 75, 104404.
- Chang, J.-S.; Wang, S.-L.; Lii, K.-H. *Inorg. Chem.* 1997, 36, 3410-3413.